Organic Geochemistry 50 (2012) 68–77

Contents lists available at SciVerse ScienceDirect

Organic Geochemistry

journal homepage: www.elsevier.com/locate/orggeochem

Archaeal tetraether lipids record subsurface water temperature in the South China Sea

Guodong Jia [a,b,*], Jie Zhang [a], Jianfang Chen [c], Ping'an Peng [b], Chuanlun L. Zhang [d,e]

[a] CAS Key Laboratory of Marginal Sea Geology, Guangzhou Institute of Geochemistry, Chinese Academy of Sciences, Guangzhou 510640, China
[b] State Key Laboratory of Organic Geochemistry, Guangzhou Institute of Geochemistry, Chinese Academy of Sciences, Guangzhou 510640, China
[c] State Key Laboratory of Satellite Ocean Environment Dynamics, Second Institute of Oceanography, SOA, Hangzhou 310012, China
[d] State Key Laboratory of Marine Geology, Tongji University, Shanghai 200092, China
[e] Department of Marine Sciences, University of Georgia, Athens, GA 30602, USA

ARTICLE INFO

Article history:
Received 9 February 2012
Received in revised form 9 July 2012
Accepted 9 July 2012
Available online 20 July 2012

ABSTRACT

The South China Sea (SCS) is the largest tropical marginal sea in the western Pacific Ocean. While the $U^{K'}_{37}$ proxy is known to reflect the sea surface temperature (SST) of the 0–30 m mixed layer in the SCS, little is known about the applicability of the TEX_{86} proxy. Here, we present results from paired analyses of TEX^{H}_{86}, a modified version of TEX_{86}, and $U^{K'}_{37}$ from core top sediment samples from the SCS. TEX^{H}_{86}-based SST calculated from the global regression exhibited slightly higher values (avg. 28.7 °C, range 27.1–30.3 °C) than values from the World Ocean Atlas 1994 (avg. 27.4 °C, range 26.1–28.6 °C) and $U^{K'}_{37}$-based temperature values (avg. 27.3 °C, range 26.1–29.0 °C). Moreover, the linear relationship between TEX^{H}_{86} and SST was poor (r^2, 0.44). Correlation analysis of TEX^{H}_{86} with annual temperature and seasonal temperature at various depths revealed that TEX^{H}_{86} correlated better with annual sea temperature at 30–125 m (r, 0.89) than with temperature in the 0–30 m mixed layer (r, 0.69). This suggests that TEX^{H}_{86} reflects a deeper and cooler subsurface temperature rather than surface or mixed layer temperature in the SCS. As a result, the global regression, which results in higher SST values, could not be applied to predict subsurface temperature in the SCS and a local calibration of TEX^{H}_{86} vs. 30–125 m subsurface temperature was tentatively established. Furthermore, the difference between $U^{K'}_{37}$ and TEX^{H}_{86} derived temperature ($\Delta T_{Alkenone-GDGT}$) correlated moderately (r, 0.62) with the depth of the thermocline of the 18 °C isotherm in the SCS, suggesting that the difference may provide a proxy for upper ocean vertical thermal gradient in this marginal sea.

1. Introduction

Reconstruction of variation in ancient sea surface temperature (SST) is essential for understanding past climate change. A range of proxies for estimating past SST has been developed, including, for example, $\delta^{18}O$ and Mg/Ca ratio of planktonic foraminifera (Emiliani, 1955; Nurnberg et al., 1996), the $U^{K'}_{37}$ proxy based on the degree of unsaturation of C_{37} alkenones (Prahl and Wakeham, 1987) and the more recent TEX_{86} proxy and its derivatives, based on glycerol dialkyl glycerol tetraethers (GDGTs) from *Archaea* (e.g. Schouten et al., 2002; Kim et al., 2008, 2010).

The $U^{K'}_{37}$ index is based on the abundance ratio of a diunsaturated C_{37} methyl alkenone and the total of di- and triunsaturated C_{37} methyl alkenones produced by a small group of haptophyte algae thriving in the mixed layer, i.e. the coccolithophore *Emiliana huxleyi* and related species (Volkman et al., 1980; Marlowe et al., 1984; Brassell et al., 1986; Conte et al., 1995). A global calibration of marine core top $U^{K'}_{37}$ values with modern surface annual mean temperature showed a linear relationship of $U^{K'}_{37} = 0.033 \times SST + 0.044$ (Müller et al., 1998), which is generally considered to be a robust SST proxy and widely used in ocean paleoclimate studies (e.g. Herbert, 2003).

Isoprenoid GDGTs are biosynthesized by *Archaea*, which occur ubiquitously in marine environments and are recognized as an important component of prokaryotes in the oceans (e.g. Karner et al., 2001; Herndl et al., 2005). These compounds contain 0–3 cyclopentyl moieties (GDGT-0 to GDGT-3) and a unique compound, thaumarchaeol (formerly crenarchaeol) (and its regio isomer), with a cyclohexyl moiety in addition to four cyclopentyl moieties (Schouten et al., 2000; Sinninghe Damsté et al., 2002). Thaumarchaeol has been postulated as a biomarker for ammonia-oxidizing *Archaea* (AOA) including marine Group I *Crenarchaeota* (de la Torre et al., 2008; Pitcher et al., 2011 and references therein) and recently placed in a new phylum, *Thaumarchaeota* (Brochier-Armanet et al., 2008; Spang et al., 2010).

Core top studies show that the relative abundances of GDGTs vary with temperature, allowing construction of a temperature

* Corresponding author at: CAS Key Laboratory of Marginal Sea Geology, Guangzhou Institute of Geochemistry, Chinese Academy of Sciences, Guangzhou 510640, China. Fax: +86 20 85290278.
E-mail address: jiagd@gig.ac.cn (G. Jia).

0146-6380/$ - see front matter © 2012 Elsevier Ltd. All rights reserved.
http://dx.doi.org/10.1016/j.orggeochem.2012.07.002

proxy called TEX_{86} (Schouten et al., 2002) according to the following formula:

$$TEX_{86} = \frac{[GDGT\text{-}2] + [GDGT\text{-}3] + [Cren']}{[GDGT\text{-}1] + [GDGT\text{-}2] + [GDGT\text{-}3] + [Cren']}$$

where Cren' is the region isomer of thaumarchaeol.

Initially, TEX_{86} was shown to correlate with SST on the basis of a relatively small set of core top sediments ($n = 44$; Schouten et al., 2002), and this was subsequently confirmed by way of mesocosm experiments (Wuchter et al., 2004; Schouten et al., 2007), marine sediment trap analysis (Wuchter et al., 2005) and more extensive global core top datasets (Kim et al., 2008). More recently, modified versions of TEX_{86}, i.e. TEX_{86}^{L} and TEX_{86}^{H}, have been proposed by Kim et al. (2010):

$$SST = 67.5 \times TEX_{86}^{L} + 46.9 \quad (r^2, 0.86,\ n = 396,\ -3\text{–}30\ ^\circ C) \qquad (1)$$

$$SST = 68.4 \times (TEX_{86}^{H} + 38.6 \quad (r^2, 0.87,\ n = 255,\ 5\text{–}30\ ^\circ C) \qquad (2)$$

where

$$TEX_{86}^{L} = \log\left(\frac{[GDGT\text{-}2]}{[GDGT\text{-}1] + [GDGT\text{-}2] + [GDGT\text{-}3]}\right)$$

$$TEX_{86}^{H} = \log TEX_{86}$$

Eq. (1) is recommended for SST < 15 °C and Eq. (2) for SST > 15 °C (Kim et al., 2010).

Although the TEX_{86} proxy has been used for reconstructing ancient SST values spanning the Cretaceous to the late Quaternary, it remains uncertain as to how well it reflects annual mean SST. For example, some studies have observed that TEX_{86} does not reflect SST, but rather subsurface temperature due to additional production of GDGTs below the mixed layer (Huguet et al., 2007; Lee et al., 2008; Lopes dos Santos et al., 2010). Other studies have shown that TEX_{86} may be biased towards summer temperature in systems such as the Eastern Mediterranean and the Adriatic Sea (Menzel et al., 2006; Castañeda et al., 2010; Leider et al., 2010) or towards winter temperature in the southern North Sea (Herfort et al., 2006) due to seasonality in growth of *Thaumarchaeota*. Moreover, marine GDGTs may also come from archaea living in the underlying sediment (Sorensen and Teske, 2006; Lipp et al., 2008; Shah et al., 2008; Lipp and Hinrichs, 2009) and in soil (Hopmans et al., 2004; Herfort et al., 2006; Kim et al., 2006; Weijers et al., 2006a,b), which would influence GDGT distributions and thus the accuracy of TEX_{86}.

Other temperature proxies have their own but distinctly different uncertainties. Application of multiple proxies to the same sediment material is one way of constraining potential uncertainty. Integrating $U_{37}^{K'}$ and TEX_{86} proxies for sediments and suspended particulates has therefore been carried out in several recent studies (Huguet et al., 2006, 2011; Lee et al., 2008; Castañeda et al., 2010; Leider et al., 2010; Lopes dos Santos et al., 2010; Caley et al., 2011; Rommerskirchen et al., 2011).

The South China Sea (SCS) is the largest tropical marginal sea in the western Pacific (Fig. 1). Intense research on SST reconstruction has been conducted for the SCS by using temperature proxies such as foraminiferal transfer function, oxygen isotope ratio values and Mg/Ca ratio of foraminifera, or $U_{37}^{K'}$ (e.g. Wei et al., 2007; Zhao et al., 2006; Jia et al., 2008; Jian et al., 2009). A detailed study has revealed a strong linear relationship for marine core top $U_{37}^{K'}$ values with annual mean temperature in the 0–30 m mixed layer (Pelejero and Grimalt, 1997):

$$U_{37}^{K'} = 0.031 \times T + 0.092 \quad (r^2, 0.86,\ n = 31,\ 0\text{–}30\ m) \qquad (3)$$

Values derived from this proxy matched the temperature at 0–30 m depth rather than that at 0 m depth (Pelejero and Grimalt, 1997; Pelejero et al., 1999). A recent study of GDGTs in the SCS showed slightly higher (ca. 1 °C) core top TEX_{86}^{H}-based SST than satellite annual SST (Wei et al., 2011). However, the values were within the prediction error (2.5 °C) for TEX_{86}^{H} and therefore considered suitable for application of TEX_{86}^{H} as an annual SST proxy in the SCS (Wei et al., 2011). However, in another study the higher core top and Holocene TEX_{86}^{H} temperature values (ca. 1.5 °C) were interpreted as reflecting warmer season temperature values (Shintani et al., 2011).

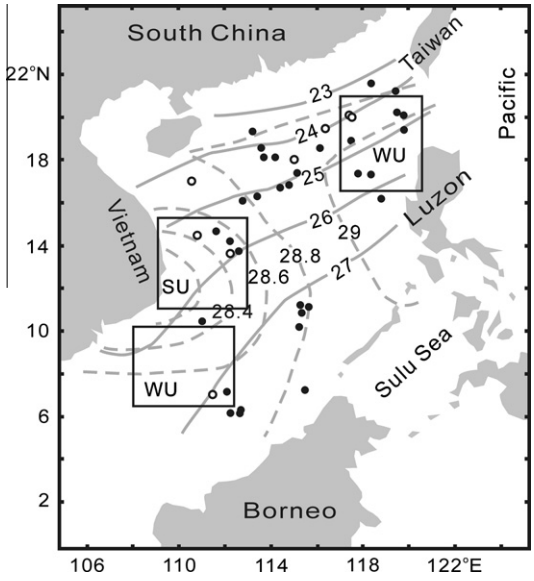

Fig. 1. Study sites and SST in the SCS. Dots are sample sites in this study and circles are those in previous studies (Shintani et al., 2011; Wei et al., 2011). Solid and dashed lines are winter and summer isotherms, respectively. The three rectangles are monsoon induced upwelling regions according to Liu et al. (2002). WU, winter upwelling; SW, summer upwelling.

In this study we have analyzed GDGT lipids in core top sediments at a water depth of 329–4182 m across the whole basin of the SCS. Most of the samples had been used for the $U_{37}^{K'}$ calibration described above (Pelejero and Grimalt, 1997). Comparison between TEX_{86}^{H} and $U_{37}^{K'}$ for the samples allowed us to evaluate how well the GDGT index reflects sea surface temperature. In particular, the coupled analysis of alkenone and GDGT proxies may shed new light on the monsoon history of the SCS.

2. Background, material and methods

The SCS is a tropical marginal sea with annual SST ranging from 25 to 29 °C. It connects with the Pacific Ocean through the 2200 m deep Luzon Strait between Taiwan Island and Luzon Island. The central deep basin has an average depth of ca. 4700 m and a maximum water depth of 5559 m, and is bordered by two broad shelves <200 m in the northern and southwestern SCS (Fig. 1).

The East Asian monsoon is the prevailing climatic feature (Wang and Li, 2009). In winter the SCS is dominated by the strong northeasterly monsoon, whereas in summer the wind becomes weak and reverses direction to southwesterly. The seasonally reversing monsoon wind plays an important role in determining the upper ocean circulation and SST patterns (Shaw and Chao, 1994). In summer, SST is uniform, varying between 28.0 and 29.5 °C; in winter, an intense western boundary current, flowing southward on the continental slope, transports cold water from the north and causes a distinct cold tongue south of Vietnam, leading to a south–north temperature gradient (Fig. 1). In most parts of the basin, there is a negative correlation (Qu, 2001) between SST and mixed layer depth, i.e. SST tends to be higher (lower) when mixed layer depth is shallower (deeper). Given the vertical

temperature gradient of 0.05 °C m^{-1} as the lowest index of the thermocline, the mixed layer depth is generally <50 m and the thermocline is thinnest and weakest in winter, thickest in spring and strongest in summer and fall (Liu et al., 2000; Qu, 2001).

The SCS is an oligotrophic region, especially towards its central part (Liu et al., 2002; Wong et al., 2007). Its biogeochemistry responds to the alternating monsoons, producing three main monsoon-driven upwelling regions (Liu et al., 2002), i.e. northwest of Luzon and north of the Sunda Shelf in winter and off the east coast of Vietnam in summer (Fig. 1).

2.1. Sample collection

A total of 32 core top sediment samples were analyzed (Fig. 1; Table 1), with 23 (#1-23, Table 1) collected during the R/V Sonne cruise in 1994 and the others (#24-32, Table 1) during a State Oceanic Administration cruise in 1998. These samples were kept refrigerated before analysis. The samples correspond to the uppermost 0–1 or 0–2 cm of box cores, assumed to represent a late Holocene timespan covering a few hundred to, at a maximum, a few thousand yr (Pelejero and Grimalt, 1997). The water depth for the cores ranges between 329 and 4182 m. Most of the samples had been used for a calibration of alkenone $U^{K'}_{37}$ vs. SST (Pelejero and Grimalt, 1997).

2.2. Methods

Each freeze-dried and homogenized sample (ca. 1 g) was ultrasonically extracted (6×) with MeOH (2×), dichloromethane (DCM)/MeOH (1:1, v/v; 2×) and DCM (2×) and all extracts were combined after centrifugation (we found that one more extraction with each solvent did not improve extraction efficiency, so the customary 3× was reduced to 2×). The bulk of the solvent was removed by way of rotary evaporation under vacuum and each total extract was purified and separated into an apolar fraction and a polar fraction over an activated silica gel column by elution with *n*-hexane and DCM/MeOH (1:1, v/v), respectively, the GDGTs being in the polar fraction. The solvent was removed under N_2 and the residue dissolved via sonication (5 min) in hexane/propanol (99:1, v/v) and filtered through a 0.45 μm, 4 mm diameter PTFE filter.

Analysis of GDGTs was performed using an Agilent 1200 HPLC/6410 TripleQuad MS instrument equipped with an auto-injector and Chemstation chromatography manager software. Procedures described by Hopmans et al. (2000) and Schouten et al. (2007)

Table 1
Station information, fractional abundance of GDGTs, TEX_{86}, BIT, MI and $U^{K'}_{37}$ values for core top samples.

No.	Station	Lon.	Lat.	Water depth (m)	Temp.[a] 0–30 (°C)	Temp.[a] 30–125 (°C)	DOT (m)	$U^{K'}_{37}$	GDGT-0	GDGT-1	GDGT-2	GDGT-3	Cren	Cren'	TEX_{86}	BIT	MI
1	17941	118.48	21.52	2201	25.91	22.76	148.5	0.9	0.2	0.059	0.078	0.011	0.597	0.056	0.71	0.14	0.18
2	17942	113.2	19.33	329	26.03	21.89	130.6	0.901	0.169	0.051	0.063	0.014	0.651	0.053	0.716	0.07	0.15
3	17943	117.55	18.95	917	26.91	22.48	133	0.917[b]	0.193	0.06	0.077	0.013	0.593	0.065	0.716	0.11	0.19
4	17944	113.64	18.66	1219	26.43	22.01	129.8	0.937	0.197	0.061	0.073	0.01	0.604	0.054	0.694	0.08	0.18
5	17945	113.78	18.13	2404	26.43	22.01	129.8	0.918[b]	0.193	0.066	0.07	0.009	0.613	0.048	0.695	0.05	0.18
6	17946	114.25	18.13	3465	26.53	22.09	129.5	0.915[b]	0.217	0.055	0.073	0.009	0.592	0.054	0.71	0.22	0.18
7	17947	116.03	18.47	3765	26.76	22.29	130.4	0.910[b]	0.2	0.063	0.086	0.012	0.575	0.065	0.709	0.07	0.2
8	17948	114.9	16.71	2841	27.18	22.43	129.3	0.937[b]	0.213	0.057	0.073	0.011	0.592	0.054	0.706	0.25	0.18
9	17949	115.17	17.35	2195	26.98	22.36	129.5	0.927[b]	0.203	0.064	0.087	0.011	0.573	0.06	0.711	0.15	0.2
10	17950	112.9	16.09	1868	26.91	22.09	128.4	0.938[b]	0.193	0.062	0.085	0.011	0.591	0.059	0.716	0.08	0.19
11	17951	113.41	16.29	2340	27.06	22.26	128.6	0.934[b]	0.183	0.057	0.077	0.01	0.625	0.049	0.704	0.09	0.18
12	17952	114.47	16.67	2864	27.18	22.43	129.2	0.938[b]	0.212	0.06	0.078	0.01	0.584	0.057	0.708	0.11	0.19
13	17954	111.53	14.8	1517	27.07	22.02	126.1	0.933[b]	0.205	0.061	0.078	0.012	0.586	0.058	0.707	0.1	0.19
14	17955	112.18	14.12	2404	27.3	22.28	126.8	0.933[b]	0.201	0.058	0.075	0.01	0.604	0.053	0.706	0.14	0.18
15	17956	112.59	13.85	3387	27.46	22.44	127.3	0.936[b]	0.213	0.062	0.085	0.01	0.571	0.059	0.712	0.25	0.2
16	17957	115.3	10.9	2197	28.27	23.75	135.4	0.968[b]	0.218	0.055	0.079	0.009	0.577	0.061	0.729	0.06	0.18
17	17958	115.08	11.62	2581	28.19	23.65	135.1	0.969[b]	0.199	0.052	0.076	0.009	0.606	0.058	0.732	0.09	0.17
18	17959	115.29	11.14	1957	28.19	23.65	135.1	0.968[b]	0.179	0.05	0.08	0.01	0.63	0.051	0.736	0.03	0.17
19	17960	115.56	10.12	1707	28.27	23.75	135.4	0.966[b]	0.179	0.052	0.077	0.01	0.633	0.049	0.734	0.06	0.17
20	17962	112.08	7.18	1970	28.21	23.68	140.9	0.956[b]	0.145	0.05	0.071	0.013	0.663	0.058	0.742	0.05	0.16
21	17963	112.67	6.17	1233	28.24	23.78	147.4	0.963[b]	0.135	0.05	0.077	0.014	0.667	0.058	0.748	0.08	0.16
22	17964	112.21	6.16	1556	28.24	23.78	147.4	0.961[b]	0.119	0.047	0.072	0.015	0.7	0.046	0.74	0.05	0.15
23	17965	112.55	6.16	889	28.24	23.78	147.4	0.972[b]	0.137	0.049	0.07	0.013	0.67	0.06	0.745	0.08	0.15
24	S031	111	10.5	2521	27.74	22.98	132.4	0.938	0.176	0.051	0.07	0.011	0.63	0.061	0.734	0.13	0.16
25	S052	115.5	7.25	1609	28.42	24.12	140.7	0.991	0.152	0.046	0.068	0.016	0.66	0.059	0.756	0.09	0.15
26	S199	118.93	16.17	3675	27.69	23.22	137.6	0.958	0.177	0.052	0.076	0.009	0.622	0.063	0.74	0.11	0.17
27	SX15	119.5	21.25	2500	26.19	23.32	163.4	0.923	0.175	0.05	0.069	0.012	0.64	0.054	0.732	0.1	0.16
28	S017	119.5	20.25	2800	26.61	23.28	158.2	0.926	0.182	0.05	0.064	0.011	0.635	0.058	0.728	0.09	0.15
29	S098	119.88	19.31	4182	26.96	23.24	152.5	0.92	0.181	0.048	0.065	0.012	0.642	0.051	0.726	0.23	0.15
30	S137	118.36	17.28	3986	27.39	22.88	136.1	0.941	0.194	0.05	0.063	0.009	0.625	0.06	0.723	0.23	0.15
31	S181	117.84	17.29	3960	27.24	22.67	132.8	0.941	0.18	0.049	0.072	0.009	0.628	0.061	0.714	0.13	0.16
32	S072	119.09	20.65	3447	26.6	23.28	158.2	0.908	0.204	0.057	0.07	0.012	0.602	0.055	0.725	0.22	0.17
33	2894	111.55	7.04	1982	28.12	23.58									0.726[c]		
34	2898	112.18	13.79	2395	27.46	22.44									0.689[c]		
35	2900	110.7	14.39	1455	26.81	21.78									0.691[c]		
36	2902	114.96	17.96	3697	26.88	22.25									0.698[c]		
37	2903	116.25	19.46	2066	26.38	22.15									0.688[c]		
38	2905	117.36	20.14	1647	26.15	22.34									0.690[c]		
39	48PC	110.53	16.96	1474	26.5	21.76									0.680[c]		
40	2146	117.38	20.12	1720	26.15	22.34									0.702[d]		

[a] Data are annual mean (provided by Physical Sciences Division, Earth System Research Laboratory, NOAA, Boulder, Colorado, from their Web site).
[b] Data are annual mean from Pelejero and Grimalt, 1997.
[c] Data are annual mean from Wei et al. (2012).
[d] Data are annual mean from Shintani et al. (2011).

were applied. Separation was achieved with a Prevail Cyano column (2.1 × 150 mm, 3 μm diameter particles; Grace, USA), maintained at 30 °C. Injection volume varied from 10 to 20 μl. GDGTs were eluted isocratically with 99% hexane and 1% propanol for 5 min, followed by a linear gradient to 1.8% propanol in 45 min. Flow rate was 0.2 ml/min. Detection was achieved using atmospheric pressure positive ion chemical ionization mass spectrometry (APCI-MS) via selected ion monotoring (SIM) of $[M+H]^+$ ions (in MS1) and GDGTs were quantified by integration of the peak areas.

For samples not included in the $U^{K'}_{37}$ work of Pelejero and Grimalt (1997), alkenones were also analyzed according to the method of Villanueva et al. (1997). Briefly, the total extract was hydrolyzed with 6% KOH/MeOH and then the hexane extract from the solution fractionated using silica column chromatography to obtain the ketone fraction, which was analyzed using a HP 6890 gas chromatograph fitted with a 30 m, 0.32 mm × 0.25 μm DB-1 column. The peak areas from the di- and tri-unsaturated C_{37} alkenones ($C_{37:2}$ and $C_{37:3}$, respectively) were used to determine the $U^{K'}_{37}$ index $[C_{37:2}/(C_{37:2} + C_{37:3})]$ as per Prahl and Wakeham (1987).

2.3. Water temperature in the upper water column

Temperature data for each station were retrieved from NODC (Levitus) World Ocean Atlas 1994 (NODC_WOA94) on a 1° grid resolution from the Web site of http://www.esrl.noaa.gov/psd/. NODC_WOA94 data provide 3 D interpolation onto 33 standardized vertical intervals from the surface (0 m) to the seafloor (5500 m), and monthly long term mean parameters between 1900 and 1992. Temperature values at 0, 10, 20, 30, 50, 75, 100, 125, 150 and 200 m were used, and seasonal temperature values were obtained as follows: Spring, March–May; Summer, June–August; Autumn, September–November; Winter, December–February.

2.4. Statistical analysis

One-way analysis of variance (ANOVA), Pearson's correlation and linear regression were performed using the software of Statistical Product and Service Solutions (SPSS) 13.0 for Windows. Statistical tests showed that data used in this work met the assumptions for normal distribution and data transformation was not conducted. The significance level or critical p value was set at 0.05. If a test of significance gave a p value < 0.05, the null hypothesis was rejected and results were considered statistically significant.

3. Results and discussion

3.1. Distribution of GDGTs

GDGTs were dominated by thaumarchaeol (61.8 ± 3.2%, n = 32) and GDGT-0 (18.5 ± 2.5%, n = 32) with the concentration of GDGT-1 to GDGT-3 and the thaumarchaeol region isomer <9%, respectively (Table 1). In the marine environment, temperature signals from GDGT-based indices may be affected by isoprenoid GDGTs produced in situ by other *Archaea* in addition to *Thaumarchaeota* (Pancost et al., 2001; Schouten et al., 2001; Wakeham et al., 2003; Zhang et al., 2011) or by GDGTs transported from land (Sinninghe Damsté et al., 2000; Weijers et al., 2006a,b). Here, the influence of other *Archaea* was examined by using two indices. One was the ratio of GDGT-0 (m/z 1302) to thaumarchaeol (m/z 1292), based on the idea that thaumarchaeol is only synthesized by *Thaumarchaeota*, whereas GDGT-0 is a common membrane lipid of *Archaea*, especially the methane-related *Archaea* (Koga et al., 1993; Pancost et al., 2001; Schouten et al., 2001). In *Thaumarchaeota* the GDGT-0/thaumarchaeol ratio is typically <2 (Schouten et al., 2002; Blaga et al., 2009) and ranged from 0.17 to 0.38 in our samples, suggesting that a contribution from *Archaea* other than *Thaumarchaeota* was insignificant. In lacustrine systems GDGT-0/thaumarchaeol can, however, be far greater than 2, indicating a strong contribution from methanogens (Blaga et al., 2009). The other index is the methane index (MI), recently proposed to quantify the relative contribution of methanotrophic *Euryarchaeota* (presumably represented by GDGT-1, -2 and -3) vs. *Thaumarchaeota* (represented by thaumarchaeol and its regio isomer) in the marine environment (Zhang et al., 2011). MI values for our samples lay in a narrow range between 0.15 and 0.20 (Table 1), well within the range of 0–0.3 for normal marine conditions assigned by Zhang et al. (2011). Therefore, contributions of GDGTs from marine *Archaea* other than *Thaumarchaeota* were neglected for our samples.

The influence of soil *Thaumarchaeota* was evaluated using the branched and isoprenoid tetraether (BIT) index, a proxy for estimating the relative contribution of soil organic matter to marine sediments (Hopmans et al., 2004; Weijers et al., 2006b). BIT values are 0.0–0.1 at the marine end and 0.8–1.0 at the soil end (Herfort et al., 2006; Weijers et al., 2006b). BIT values for our samples averaged 0.12 ± 0.06 (n = 32) and ranged from 0.03 to 0.25, suggesting a predominantly marine source (Table 1). The potential effect of soil derived GDGTs on the TEX_{86} proxy was also assessed by correlating BIT values with TEX_{86} values, as suggested by Schouten et al. (2009). This was carried out and no significant correlation was found. The temperature signals from GDGT-based indices from our samples are therefore unlikely to be biased significantly by the presence of soil derived GDGTs.

3.2. TEX^H_{86} derived temperature from global regression

According to Kim et al. (2010), the thaumarchaeol regio isomer is strongly correlated with SST at high values but not at low SST values. It was therefore concluded that TEX^H_{86} is better suited for the determination of SST in (sub)tropical oceans, whereas TEX^L_{86}, not containing the thaumarchaeol regio isomer, is more appropriate for (sub)polar oceans, where the concentration of the regio isomer is often relatively low. In our study, the thaumarchaeol regio isomer content was comparable to that of GDGTs 1–3 (Table 1), and we found that the annual mean temperature at every water depth, i.e. 0, 10, 20, 30, 50, 75, 100, 125, 150 and 200 m, correlated better with TEX^H_{86} (r, 0.50–0.89) than with TEX^L_{86} (r, 0–0.66). Additionally, SST values calculated from TEX_{86} index ($SST = 56.2 \times TEX_{86} - 10.78$; Kim et al., 2008) was higher (2.0 ± 0.9 °C) than NODC SST, which means higher residuals from TEX_{86} prediction than from TEX^H_{86} prediction (1.2 ± 0.7 °C; see next paragraph). Therefore, consistent with the suggestion of using TEX^H_{86} in (sub)tropical oceans (Kim et al., 2010), TEX^H_{86} also seems to be more suitable for the (sub)tropical SCS. The following discussion therefore focuses on TEX^H_{86} derived SST [Eq. (2)]. In addition, recently reported TEX^H_{86} values for eight core top samples collected from the SCS by other authors (#33-40 in Table 1; Shintani et al., 2011; Wei et al., 2011) were combined with our data in the discussion. In addition, a second SST proxy, $U^{K'}_{37}$ was employed for comparison [Eq. (3)].

As shown in Fig. 2a, TEX^H_{86} derived SST is higher on average (1.2 ± 0.7 °C) than the NODC SST, whereas the $U^{K'}_{37}$ derived temperature is more consistent with the NODC SST. The difference of 1.2 ± 0.7 °C between TEX^H_{86} derived SST and NODC SST is less than the calibration error for TEX^H_{86}, which is 2.5 °C (Kim et al., 2010). So, TEX^H_{86} seems to predict SST within the error of the proxy. Indeed, SCS data lie close to the upper end of the global regression (Fig. 3a). However, ANOVA analysis performed on the residuals of SST estimates of TEX^H_{86} (i.e. the difference between TEX^H_{86} SST and NODC SST) indicated that the difference between the global (Kim

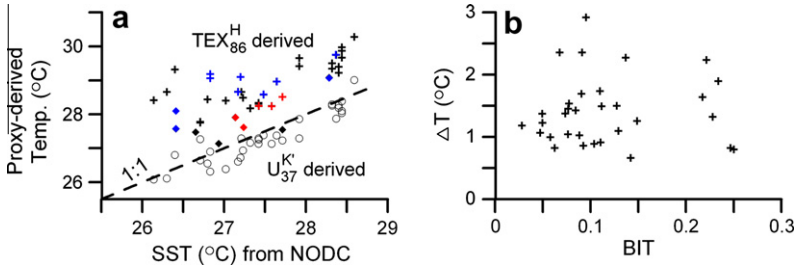

Fig. 2. (a) Comparison of temperature estimates from TEX_{86}^{H} [Eq. (2)], $U_{37}^{K'}$ [Eq. (3)] and NODC SSTs in the SCS. Cross, this study; diamond, Shintani et al. (2011) and Wei et al. (2011); blue, sample site in the winter upwelling region; red, sample site in the summer upwelling region. (b) Difference between TEX_{86}^{H} derived temperatures and NODC SSTs (ΔT), and relationship with BIT index. (For interpretation of the references to color in this figure legend, the reader is referred to the web version of this article.)

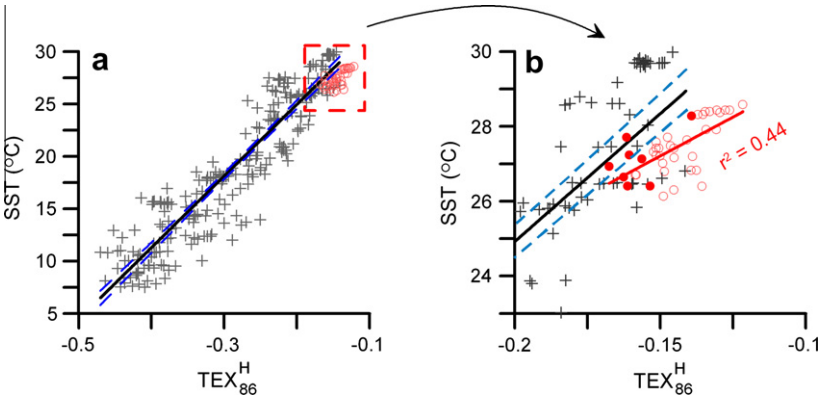

Fig. 3. Comparison of SCS data set (red circles) with global data set (gray crosses). (b) Is a closer inspection of (a). Black lines are global regressions given by Kim et al. (2010) and red line is regression for the SCS data set. The dashed lines are 95% confidence intervals for the global regressions. Red dots in (b) are data from Shintani et al. (2011) and Wei et al. (2011). (For interpretation of the references to color in this figure legend, the reader is referred to the web version of this article.)

et al., 2010) and SCS data was statistically significant ($F = 10.8$, $p < 0.05$). Closer examination reveals that SCS data deviate from the global calibration and can generate a quite different regression line of SST at 0 m vs. TEX_{86}^{H}, but with a relatively low r^2 value (0.44 in Fig. 3b). Therefore, the consistently higher TEX_{86}^{H} derived SST and poor correlation between SST at 0 m and TEX_{86}^{H} imply that TEX_{86}^{H} derived SST is less precise than $U_{37}^{K'}$ derived values for the SCS. In the following sections, possible causes for this are discussed.

One explanation for the higher TEX_{86}^{H} SST than both NODC and $U_{37}^{K'}$ SST in the SCS could be due to the possible contamination of marine GDGTs by soil derived GDGTs and/or lateral sediment transport from different areas. The possibility of soil derived GDGTs was ruled out due to the lack of correlation between BIT values and TEX_{86} values (see above). In addition, the TEX_{86}^{H} NODC temperature difference and BIT were also not correlated (Fig. 2b), suggesting that interference from soil derived GDGTs is not likely the main cause of the temperature difference. Lateral transport has been shown to affect alkenones more than GDGTs due to the less refractory nature of GDGTs relative to alkenones (Mollenhauer et al., 2007, 2008; Shah et al., 2008). So, GDGT-based proxies were suggested to be primarily influenced by local conditions and less subject to long distance lateral transport (Kim et al., 2010). Although $U_{37}^{K'}$ temperature estimates have been found at variance with in situ SST in some areas due to lateral transport (e.g. Benthien and Müller, 2000; Mollenhauer et al., 2006), the consistency between $U_{37}^{K'}$ temperature and NODC SST in this study indicates its minor effect on the $U_{37}^{K'}$ proxy in the SCS. The smallest ^{14}C offsets between alkenones and planktonic foraminifera found in the SCS relative to other areas (Shah et al., 2008) also support the minimum effect of lateral transport in the SCS.

Secondly, the warmer TEX_{86}^{H} temperature could indicate that TEX_{86}^{H} SST might be biased toward warmer season temperature if the source organisms thrive in warmer seasons. This scenario has been used to interpret the higher TEX_{86}^{H} SST than $U_{37}^{K'}$ SST in surface and downcore sediments (Castañeda et al., 2010; Leider et al., 2010; Shintani et al., 2011). Several authors have noticed that seasonal differences in thaumarchaeotal production may account for part of the scatter in the relationship for TEX_{86} vs. annual mean temperature (Herfort et al., 2006; Wuchter et al., 2006; Kim et al., 2010). Indeed, our data show varying correlation coefficients between TEX_{86}^{H} and seasonal water temperature, but the lowest r value (<0.3) for TEX_{86}^{H} with summer SST does not support the idea of warmer season-biased TEX_{86}^{H} SST (Fig. 4a). On the other hand, the marked low r values at 0 and 10 m depth (r, 0.26 and 0.41, respectively) in summer (Fig. 4a) do not suggest TEX_{86}^{H} bias against summer temperature, but might be associated with the small temperature difference (<0.8 °C) for this season that is difficult to distinguish using the TEX_{86}^{H} index. In addition, samples located in winter or summer upwelling regions (Fig. 1a) do not stand out from others in the cross plot of TEX_{86}^{H} SST vs. $U_{37}^{K'}$ SST (Fig. 2a), suggesting that the warmer TEX_{86}^{H} values were not associated with temporal and spatial changes in phytoplankton bloom, although *Thaumarchaeota* have been observed to be offset either in space or time from the main phytoplankton bloom (Massana et al., 1997; Murray et al., 1998, 1999). However, the lack of information on the seasonal abundances of marine *Thaumarchaeota* and on GDGT flux in the water column of the SCS does not allow us to confidently address this question at present. Nevertheless, we found that sedimentary TEX_{86}^{H} values exhibit (Fig. 4a) a strong correlation with annual temperature at every water depth (r from 0.55 to 0.88 over the depth range between 0 and 200 m), suggesting that TEX_{86}^{H} is not seasonally biased. This suggestion is consistent with the findings for the Arabian Sea where the GDGT temperature signal in sediment traps at 1500 m and 3000 m did not show the seasonal

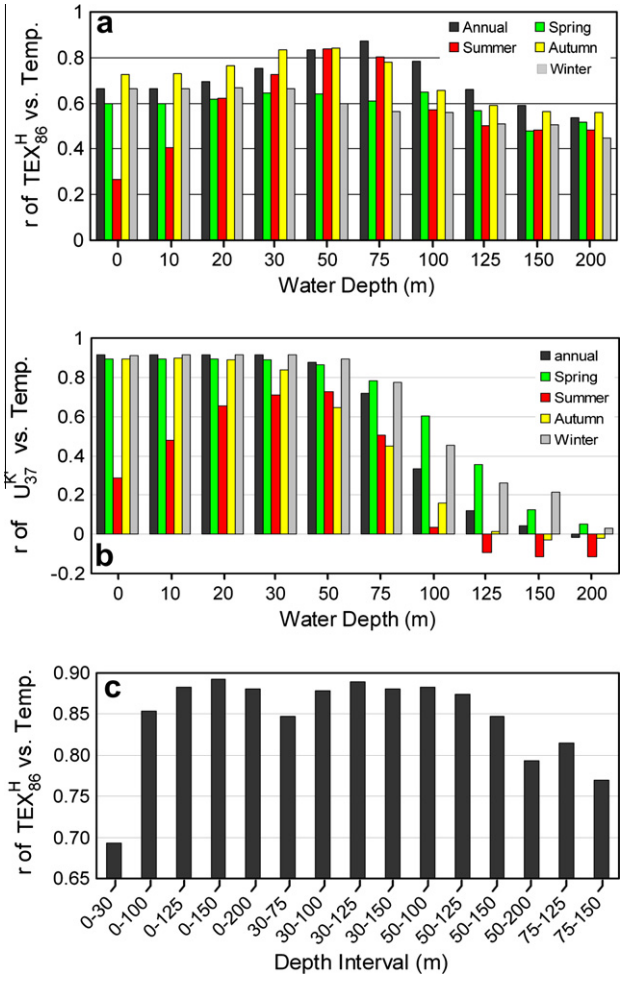

Fig. 4. Correlation coefficient (r value) of seasonal and annual water column temperature vs. TEX_{86}^{H} and $U_{37}^{K'}$ indices. Temperatures for depth intervals in (c) were calculated according to Eq. (4) in the text.

cyclicity observed in the 500 m trap, but rather reflected the annual mean SST. This was explained as resulting from homogenization of the GDGT temperature signal carried by particles as they ultimately reach the interior of the ocean (Wuchter et al., 2006). Therefore, growth of the source organisms in warmer seasons is unlikely to be the cause of the observed warmer TEX_{86}^{H} SST in the SCS.

A third explanation might relate to the water depth at which the source organisms live, which has been invoked to interpret differences between GDGTs-based temperature for SST and alkenone-based temperature (Huguet et al., 2007; Lopes dos Santos et al., 2010). However, in previous studies, the TEX_{86}^{H} temperature values were lower and attributed to a contribution from a subsurface signal. We noticed that, in the upper water column (0–200 m) in the SCS, TEX_{86}^{H} correlates strongly ($r > 0.78$) with the annual mean temperature at 50–100 m depth, whereas $U_{37}^{K'}$ correlates most strongly ($r > 0.88$) with annual mean temperature at a water depth of 50 m and shallower (Fig. 4a and b). The different patterns suggest that the two proxies reflect water temperature at different depths, i.e. TEX_{86}^{H} reflects a deeper and cooler subsurface temperature whereas $U_{37}^{K'}$ reflects a temperature for the mixed layer (<50 m depth; Qu, 2001). Recently, depth profiles of gene signatures of *Thaumarchaeota*, including 16S rRNA genes and *amo*A gene encoding key enzymes of ammonia oxidation, were investigated in the SCS (Hu et al., 2011). The data showed that the abundance of the *amo*A genes was low near the surface (5 m), increased with depth to maximal values at 50–200 m, and deceased again in bottom water (>2000 m). Moreover, the average density of copepods has been found to be higher in samples collected from 0 to 100 m and 0 to 150 m than that in surface samples in the SCS (Hwang et al., 2010), suggesting that zooplankton grazing could be higher in subsurface water, thereby providing a potential mechanism for delivery of subsurface isoprenoid GDGT lipids to the sediment. This vertical pattern of *Thaumarchaeota* gene abundance and zooplankton density suggests that temperature signals from planktonic archaea at the subsurface may be delivered smoothly to the sediment and hence may contribute predominantly to the TEX_{86}^{H} derived temperature for the sediments of the SCS. However, this scenario contradicts the observed warmer TEX_{86}^{H} temperature values calculated from Eq. (2) here. It also differs from other studies where the subsurface temperature signal was asserted to by way of lower TEX_{86}-based values than the corresponding surface temperature values (e.g. Huguet et al., 2007; Lopes dos Santos et al., 2010). Since TEX_{86}^{H} correlated poorly with SST at 0 m but was positively correlated with the temperature at 75 m (r, 0.87), we hypothesize that a regional calibration of TEX_{86}^{H} vs. subsurface temperature should be more precise than the global one for the SCS, as discussed in the following sections.

3.3. Calibration of TEX_{86}^{H} in the SCS

The better correlation between TEX_{86}^{H} and water temperature at 75 m (Fig. 4a) suggests that the temperature signals recorded via TEX_{86}^{H} may derive from subsurface water centering around 75 m. Testing this may allow us to develop a new calibration for TEX_{86}^{H} in the SCS. In order to do this, a comparison between TEX_{86}^{H} and annual mean temperature at different water depth intervals was carried out (Fig. 4c). The annual mean temperature for a particular depth interval, e.g. mean temperature from 30 to 100 m, was defined as follows, according to Kim et al. (2008):

$$\begin{aligned}\mathrm{Temp}_{\cdot 30-100\ \mathrm{m}} = [&(20 \times (\mathrm{Temp}_{\cdot 30\ \mathrm{m}} + \mathrm{Temp}_{\cdot 50\mathrm{m}})/2)\\ &+(25 \times (\mathrm{Temp}_{\cdot 50\mathrm{m}} + \mathrm{Temp}_{\cdot 75\mathrm{m}})/2)\\ &+(25 \times (\mathrm{Temp}_{\cdot 75\mathrm{m}} + \mathrm{Temp}_{\cdot 100\mathrm{m}})/2)]/70 \end{aligned} \quad (4)$$

Here, Temp. with a subscript (e.g. 30 m), denotes the water temperature at the depth in question. Our results reveal the highest r value (0.893) for the 0–150 m interval (Fig. 4c), consistent with work showing that TEX_{86} is an appropriate indicator of epipelagic sea temperature (Kim et al., 2008). Then, a regression line between 0 and 150 m annual mean temperature and TEX_{86}^{H} was obtained as follows (Fig. 5a):

$$T = (49.1 \pm 8.1) \times TEX_{86}^{H} + (30.0 \pm 1.2) \quad (r^2, 0.80,\ n = 40,\ p \ll 0.001,\ 0\text{—}150\ \mathrm{m})$$

However, from our results, the r value of 0.693 for TEX_{86}^{H} vs. the 0–30 m depth interval is apparently lower than those for other depth intervals (Fig. 4c), and the correlation between TEX_{86}^{H} and 30–125 m temperature (r, 0.889) is nearly identical to the best correlation of TEX_{86}^{H} vs. 0–150 m (r, 0.893). This observation is in contrast to the results of Kim et al. (2008) showing that TEX_{86} correlates better with the 0 m temperature than with the 0–200 m temperature. Given the poor correlation of TEX_{86}^{H} vs. 0–30 SST and the low gene abundance of *Thaumarchaeota* in surface water in the SCS (Hu et al., 2011), the 0–150 m temperature signal of TEX_{86}^{H} can be further refined to the 30–125 m subsurface temperature. Thus, the following regression line can be obtained (Fig. 5b):

$$T_{sub} = (54.5 \pm 9.2) \times TEX_{86}^{H} + (30.7 \pm 1.3) \quad (r^2, 0.79,\ n = 40,\ p \ll 0.001, 30\text{—}125\ \mathrm{m})$$

The standard error of the residuals using the above linear regression is 0.3 °C (Fig. 5c). This value is much lower than the 2.5 °C based on

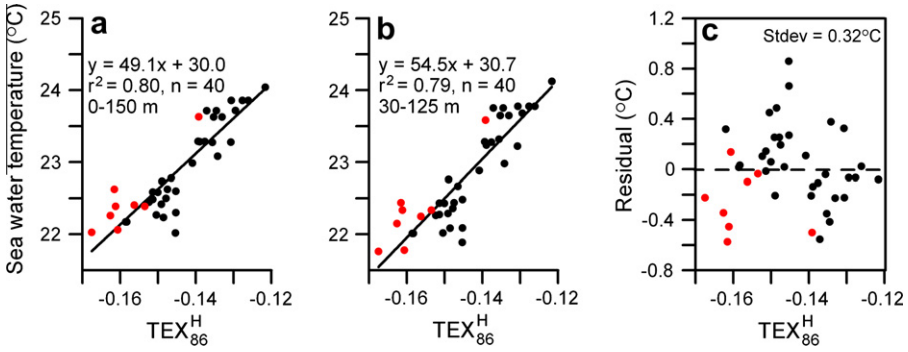

Fig. 5. Relationship between TEX_{86}^{H} and water column temperature at (a) 0–150 m and (b) 30–125 m; (c) residuals of estimates from regression of 30–125 m temperature vs. TEX_{86}^{H}. Red dots are data from Shintani et al. (2011) and Wei et al. (2011). (For interpretation of the references to color, the reader is referred to the web version of this article.)

the global regression (Kim et al., 2010), indicating that the new calibration is more precise for temperature reconstruction in the SCS.

We noticed that the use of TEX_{86} index as an indicator of subsurface temperature has been performed for other regions (Huguet et al., 2007; Lopes dos Santos et al., 2010). However, in those applications, the equation established for SST estimates, i.e. Eq. (2), was used for subsurface temperature calculation. Our findings differ from those studies in that a new equation was established for subsurface temperature estimates in the SCS following the observation that TEX_{86}^{H} correlated more strongly with subsurface temperature than with SST. The different equation for the SCS might suggest that *Thaumarchaeota* in the SCS are genetically different than those in most other places, similar to findings for the Red Sea (Ionescu et al., 2009; Trommer et al., 2009). A recent SCS study showed that the community structures of planktonic *Archaea* varied with depth, with decreasing heterotrophic metabolism of *Thaumarchaeota* in the meso- or bathypelagic zones, in contrast to observations for the North Atlantic Ocean (Agogué et al., 2008) and Eastern Mediterranean Sea (De Corte et al., 2009). However, little is known about the genetic character of *Thaumarchaeota* in the SCS and, unlike the highly isolated Red Sea, the SCS is open to the Pacific through the Luzon strait (sill depth 2200 m), and does not stand out as being unique in terms of temperature or salinity. Further study is clearly needed to explore the possibility of genetically different *Thaumarchaeota* in the SCS.

On the other hand, the different equation proposed here does not necessarily indicate unique *Thaumarchaeota* in the SCS. The poor relationship between TEX_{86}^{H} and SST in the SCS could be caused by the much narrower temperature range (26.1–28.6 °C) and smaller dataset for this study of the SCS relative to the larger range represented in the global calibration. In fact, the SCS data can fit modestly into the global data, as illustrated in Fig. 2a. Similar cases can also occur when a subset of the global dataset (Kim et al., 2010) is extracted and reduced to a narrower SST range, e.g. 25–30 °C, where the linear relationship between TEX_{86}^{H} and SST would be quite different from Eq. (2) with an r^2 value of only 0.34 (data not illustrated). In the global equation, the range of SST values may conceal important regional factors, including season and depth of GDGT production, regional variability in allochthonous and autochthonous contribution and differential susceptibility to decomposition during transport. The narrow SST range in the SCS is similar to the global calibration error of 2.5 °C, implying that the global calibration would not precisely predict SST change in the SCS. When regional variability is important, the error in the global calibration for the region is maximized. But regional factors are more likely to be constant over time in a single location than across the whole global data set (Shevenell et al., 2011). Therefore, we argue that a regional calibration is appropriate for the SCS, where a rather narrow range of temporal and spatial sea temperature occurred in the past (<4 °C during glacial–interglacial cycles; Jia et al., 2006). Nevertheless, our calibration is based solely on core top samples, which might be a few hundreds or thousands yr old (Pelejero and Grimalt, 1997) and would influence the relationship observed with modern SST. In addition, modeled temperature values, not measured ones, were used in our calibration, which could cause additional uncertainty. Thus, additional studies that investigate the vertical and temporal distribution of temperature and GDGT lipids in both suspended particulate matter from the water column at different times in the annual cycle and multi-yr long record of settling particles in sediment traps at different depths, are needed before the relationships documented in this study can be firmly established.

3.4. Implications for reconstruction of upper ocean vertical thermal gradient

The vertical thermal gradient in the upper ocean, intimately related to the depth of the thermocline (DOT), is of particular importance for the tropical Pacific and the SCS because the vertical thermal gradient is linked closely with the El Niño-Southern Oscillation (ENSO) and the East Asian monsoon. Until now, reconstruction of the vertical thermal gradient for the upper ocean or DOT has been determined by analyzing surface and subsurface planktonic foraminifers, including their assemblages, transfer functions and $\delta^{18}O$ values (Jian et al., 2009). As the thermocline becomes shallower, the difference between surface and subsurface foram parameters increases (Ravelo and Shackleton, 1995). Similarly, we suggest that the difference between $U_{37}^{K'}$ and TEX_{86}^{H} derived temperature values ($\Delta T_{Alkenone-GDGT}$) may be used for reconstructing the upper ocean vertical thermal gradient in the SCS because, as discussed above, $U_{37}^{K'}$ and TEX_{86}^{H} indices predominantly reflect the 0–30 m mixed layer temperature and the 30–125 m subsurface temperature, respectively. Recently, this method was used by Lopes dos Santos et al. (2010) to reconstruct vertical thermal gradients in the eastern tropical North Atlantic.

To test this hypothesis, we examined the relationship between DOT values and $\Delta T_{Alkenone-GDGT}$ values for the study sites in the SCS. The annual average DOT was defined as the 18 °C isothermal depth (Houghton, 1991) and was determined by a cubic spline fit of the temperature data available (Andreasen and Ravelo, 1997) from the NOAA National Oceanographic Data Center (NODC). Calculated values of DOT for our sites range from 126 m to 163 m and average 137 ± 10 m (Table 1). Values for $\Delta T_{Alkenone-GDGT}$ from surface sediments vary between 3.3 °C and 5.5 °C, with a mean value of 4.4 ± 0.6 °C. As expected, the cross plot of DOT vs. $\Delta T_{Alkenone-GDGT}$ (Fig. 6) shows a significant trend of shoaling of the DOT with the increase in difference between surface and subsurface temperatures, demonstrating that $\Delta T_{Alkenone-GDGT}$ is indeed a reasonable

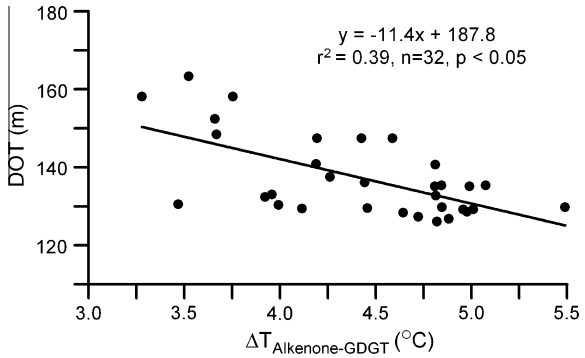

Fig. 6. Relationship between $U^{K'}_{37}$ and TEX^{H}_{86} derived temperatures ($\Delta T_{Alkenone-GDGT}$) with depth of thermocline (DOT) defined as 18 °C isothermal depth. $U^{K'}_{37}$ temperature represents 0–30 mixed layer estimate and TEX^{H}_{86} temperature represents 30–125 subsurface estimate.

proxy for reconstruction of DOT in the SCS, or the upper ocean vertical thermal gradient. This result suggests a new method for DOT reconstruction, and has the potential to strengthen multi-proxy approaches for paleoclimate and paleoceanographic studies. However, in the cross plot of DOT vs. $\Delta T_{Alkenone-GDGT}$ the data points are scattered and the r^2 value of the regression line is not high (Fig. 6). We speculate that some of the scattering might be caused by ecological factors such as seasonal differences and varying depth of archaeal and coccolithophores production, which should be resolved in future studies. Moreover, because our calibration is based solely on core top samples and modeled sea water temperature rather than in situ water column measurements, water column studies should be carried out to test whether or not the $\Delta T_{Alkenone-GDGT}$ can be a robust proxy for DOT reconstruction for the SCS in the future.

4. Conclusions

In the SCS, TEX^{H}_{86} temperature calculated from the global calibration exhibited slightly higher values (1.2 ± 0.7 °C) than the actual SST and the corresponding $U^{K'}_{37}$ temperature. Our data showed that TEX^{H}_{86} correlated better with the 30–125 m subsurface temperature (r, 0.91) than with the 0–30 m SST (r, 0.70), suggesting that the TEX^{H}_{86} proxy is influenced by the subsurface water depth at which the source organisms (*Thaumarchaeota*) live. Therefore, a new local calibration of TEX^{H}_{86} vs. 30–125 m subsurface temperature was proposed, which may be useful for subsurface temperature reconstruction in paleoceanographic studies of the SCS. TEX^{H}_{86} for the SCS contrasted with $U^{K'}_{37}$, which reflected the 0–30 mixed layer temperature. Decoupling the temperature signals from TEX^{H}_{86} and $U^{K'}_{37}$ indices thus may provide a novel approach for the reconstruction of upper ocean vertical thermal gradient, which is conventionally achieved from surface and subsurface foraminiferal analysis. Because the timing and spacing of marine *Thaumarchaeota* production are usually controlled by local factors, the applicability of TEX^{H}_{86} index as an indicator of subsurface temperature to other oceanic settings remains to be investigated.

Acknowledgements

Samples were collected during R/V SONNE cruise in 1994 and during a SOA cruise in 1998. The work is supported by the National Basic Research Program of China (No. 2009CB421206) and the NSF of China (91128212). C.L.Z. is funded by the NSF of China (91028005) and the State Key Laboratory of Marine Geology at Tongji University. We are grateful to two anonymous reviewers for thoughtful reviews. This is contribution No. IS-1536 from GIGCAS.

Associate Editor—**E.A. Canuel**

References

Agogué, H., Brink, M., Dinasquet, J., Herndl, G.J., 2008. Major gradients in putatively nitrifying and non-nitrifying archaea in the deep North Atlantic. Nature 456, 788–791.

Andreasen, D.J., Ravelo, A.C., 1997. Tropical Pacific Ocean thermocline depth reconstructions for the last glacial maximum. Paleoceanography 12, 395–413.

Benthien, A., Müller, P.J., 2000. Anomalously low alkenone temperatures caused by lateral particle and sediment transport in the Malvinas Current region, western Argentine Basin. Deep-Sea Research I 47, 2369–2393.

Blaga, C.I., Reichart, G.J., Heiri, O., Sinninghe Damsté, J.S., 2009. Tetraether membrane lipid distributions in water-column particulate matter and sediments: a study of 47 European lakes along a north–south transect. Journal of Paleolimnology 41, 523–540.

Brassell, S.C., Eglinton, G., Marlowe, I.T., Pflaumann, U., Sarnthein, M., 1986. Molecular stratigraphy: a new tool for climatic assessment. Nature 320, 129–133.

Brochier-Armanet, C., Boussau, B., Gribaldo, S., Forterre, P., 2008. Mesophilic crenarchaeota: proposal for a third archaeal phylum, the Thaumarchaeota. Nature Reviews Microbiology 6, 245–252.

Caley, T., Kim, J.-H., Malaizé, B., Giraudeau, J., Laepple, T., Caillon, N., Charlier, K., Rebaubier, H., Rossignol, L., Castañeda, I.S., Schouten, S., Sinninghe Damsté, J.S., 2011. High-latitude obliquity as a dominant forcing in the Agulhas current system. Climate of the Past 7, 1285–1296.

Castañeda, I.S., Schefuß, E., Pätzold, J., Sinninghe Damsté, J.S., Weldeab, S., Schouten, S., 2010. Millennial-scale sea surface temperature changes in the eastern Mediterranean (Nile River Delta region) over the last 27,000 years. Paleoceanography 25, PA1208. http://dx.doi.org/10.1029/2009PA001740.

Conte, M.H., Thompson, A., Eglinton, G., Green, J.C., 1995. Lipid biomarker diversity in the coccolithophorid *Emiliania huxleyi* (prymnesiophyceae) and the related species *Gephyrocapsa oceanica*. Journal of Phycology 31, 272–281.

De Corte, D., Yokokawa, T., Varela, M.M., Agogue, H., Herndl, G.J., 2009. Spatial distribution of bacteria and archaea and amoA gene copy numbers throughout the water column of the Eastern Mediterranean Sea. The ISME Journal 3, 147–158.

de la Torre, J.R., Walker, C.B., Ingalls, A.E., Konneke, M., Stahl, D.A., 2008. Cultivation of a thermophilic ammonia oxidizing archaeon synthesizing crenarchaeol. Environmental Microbiology 10, 810–818.

Emiliani, C., 1955. Pleistocene temperatures. Journal of Geology 63, 538–578.

Herbert, T.D., 2003. Alkenone paleotemperature determinations. In: Elderfield, H. (Ed.), The Oceans and Marine Geochemistry, vol. 6. In: Holland, H.D., Turekian, K.K. (Eds.), Treatise on Geochemistry. Elsevier-Pergamon, Oxford, pp. 391–432.

Herfort, L., Schouten, S., Boon, J.P., Sinninghe Damsté, J.S., 2006. Application of the TEX_{86} temperature proxy in the southern North Sea. Organic Geochemistry 37, 1715–1726.

Herndl, G.J., Reinthaler, T., Teira, E., Van Aken, H., Veth, C., Pernthaler, A., Pernthaler, J., 2005. Contribution of Archaea to total prokaryotic production in the deep Atlantic Ocean. Applied and Environental Microbiology 71, 2303–2309.

Hopmans, E.C., Schouten, S., Pancost, R.D., Van der Meer, M.T.J., Sinninghe Damsté, J.S., 2000. Analysis of intact tetraether lipids in archaeal cell material and sediments by high performance liquid chromatography/atmospheric pressure chemical ionization mass spectrometry. Rapid Communications in Mass Spectrometry 14, 585–589.

Hopmans, E.C., Weijers, J.W.H., Schefuß, E., Herfort, L., Sinninghe Damsté, J.S., Schouten, S., 2004. A novel proxy for terrestrial organic matter in sediments based on branched and isoprenoid tetraether lipids. Earth and Planetary Science Letters 224, 107–116.

Houghton, R.W., 1991. The relationship of sea surface temperature to thermocline depth at annual and interannual time scales in the tropical Atlantic Ocean. Journal of Geophysical Research 96, 15173–15185.

Hu, A.Y., Jiao, N.Z., Zhang, C.L., 2011. Community structure and function of planktonic Crenarchaeota: changes with depth in the South China Sea. Microbial Ecology 62, 549–563.

Huguet, C., Kim, J.-H., Sinninghe Damsté, J.S., Schouten, S., 2006. Reconstruction of sea surface temperature variations in the Arabian Sea over the last 23 kyr using organic proxies (TEX_{86} and $U^{K'}_{37}$). Paleoceanography 21, PA3003. http://dx.doi.org/10.1029/2005PA001215.

Huguet, C., Schimmelmann, A., Thunell, R., Lourens, L.J., Sinninghe Damsté, J.S., Schouten, S., 2007. A study of the TEX_{86} paleothermometer in the water column and sediments of the Santa Barbara Basin, California. Paleoceanography 22, PA3202. http://dx.doi.org/10.1029/2006PA001310.

Huguet, C., Martrat, B., Grimalt, J.O., Sinninghe Damsté, J.S., Schouten, S., 2011. Coherent millennial-scale patterns in $U^{K'}_{37}$ and TEX^{H}_{86} temperature records during the penultimate interglacial-to-glacial cycle in the western Mediterranean. Paleoceanography 26, PA2218. http://dx.doi.org/10.1029/2010PA002048.

Hwang, J.-S., Kumar, R., Dahms, H.-U., Tseng, L.-C., Chen, Q.-C., 2010. Interannual, seasonal, and diurnal variations in vertical and horizontal distribution patterns

of 6 *Oithona* spp. (Copepoda: Cyclopoida) in the South China Sea. Zoological Studies 49, 220–229.
Ionescu, D., Penno, S., Haimovich, M., Rihtman, B., Goodwin, A., Schwartz, D., Hazanov, L., Chernihovsky, M., Post, A.F., Oren, A., 2009. Archaea in the Gulf of Aqaba. FEMS Microbiology Ecology 69, 425–438.
Jia, G.D., Xie, H.Q., Peng, P.A., 2006. Contrast in surface water $\delta^{18}O$ distributions between the Last Glacial Maximum and the Holocene in the Southern South China Sea. Quaternary Science Reviews 25, 1053–1064.
Jia, G.D., Chen, F.J., Peng, P.A., 2008. Sea surface temperature differences between the western equatorial Pacific and northern South China Sea since the Pliocene and their paleoclimatic implications. Geophysical Research Letters 35, L18609. http://dx.doi.org/10.1029/2008GL034792.
Jian, Z.M., Tian, J., Sun, X.J., 2009. Upper water structure and paleo-monsoon. In: Wang, P., Li, Q. (Eds.), The South China Sea, Developments in Paleoenvironmental Research, vol. 13. Springer Science+Business, Media B.V., pp. 297–394, doi: http://dx.doi.org/10.1007/978-1-4020-9745-45.
Karner, M.B., DeLong, E.F., Karl, D.M., 2001. Archaeal dominance in the mesopelagic zone of the Pacific Ocean. Nature 409, 507–510.
Kim, J.-H., Schouten, S., Buscail, R., Ludwig, W., Bonnin, J., Sinninghe Damsté, J.S., Bourrin, F., 2006. Origin and distribution of terrestrial organic matter in the NW Mediterranean (Gulf of Lions): exploring the newly developed BIT index. Geochemistry Geophysics Geosystems 7, Q11017. http://dx.doi.org/10.1029/2006GC001306.
Kim, J.-H., Schouten, S., Hopmans, E.C., Donner, B., Sinninghe Damsté, J.S., 2008. Global sediment core-top calibration of the TEX_{86} paleothermometer in the ocean. Geochimica et Cosmochimica Acta 72, 1154–1173.
Kim, J.-H., van der Meer, J., Schouten, S., Helmke, P., Willmott, V., Sangiorgi, F., Koç, N., Hopmans, E.C., Sinninghe Damsté, J.S., 2010. New indices and calibrations derived from the distribution of crenarchaeal isoprenoid tetraether lipids: implications for past sea surface temperature reconstructions. Geochimica et Cosmochimica Acta 74, 4639–4654.
Koga, Y., Akagawa-Matsusita, M., Ohga, M., Nishihara, M., 1993. Taxonomic significance of the distribution of component parts of polar ether lipids in methanogens. Systematic and Applied Microbiology 16, 342–351.
Lee, K.E., Kim, J.-H., Wilke, I., Helmke, P., Schouten, S., 2008. A study of the alkenones, TEX_{86}, and planktonic foraminifera in the Benguela Upwelling System: implications for past sea surface temperature estimates. Geochemistry Geophysics Geosystems 9, Q10019. http://dx.doi.org/10.1029/2008GC002056.
Leider, A., Hinrichs, K.-U., Mollenhauer, G., Versteegh, G.J.M., 2010. Core-top calibration of the lipid-based $U^{K'}_{37}$ and TEX_{86} temperature proxies on the southern Italian shelf (SW Adriatic Sea, Gulf of Taranto). Earth and Planetary Science Letters 300, 112–124.
Lipp, J.S., Hinrichs, K.-U., 2009. Structural diversity and fate of intact polar lipids in marine sediments. Geochimica et Cosmochimica Acta 73, 6816–6833.
Lipp, J.S., Morono, Y., Inagaki, F., Hinrichs, K.-U., 2008. Significant contribution of Archaea to extant biomass in marine subsurface sediments. Nature 454, 991–994.
Liu, Q., Yang, H., Wang, Q., 2000. Dynamic characteristics of seasonal thermocline in the deep sea region of the South China Sea. Chinese Journal of Oceanology and Limnology 18, 104–109.
Liu, K.-K., Chao, S.-Y., Shaw, P.-T., Gong, G.-C., Chen, C.-C., Tang, T.Y., 2002. Monsoon-forced chlorophyll distribution and primary production in the South China Sea: observations and a numerical study. Deep-Sea Research I 49, 1387–1412.
Lopes dos Santos, R.A., Prange, M., Castaneda, I.S., Schefuss, E., Mulitza, S., Schulz, M., Niedermeyer, E.M., Sinninghe Damsté, J.S., Schouten, S., 2010. Glacial–interglacial variability in Atlantic meridional overturning circulation and thermocline adjustments in the tropical North Atlantic. Earth and Planetary Science Letters 300, 407–414.
Marlowe, I.T., Brassell, S.C., Eglinton, G., Green, J.C., 1984. Long-chain unsaturated ketones and esters in living algae and marine sediments. Organic Geochemistry 6, 135–141.
Massana, R., Murray, A.E., Preston, C.M., DeLong, E.F., 1997. Vertical distribution and phylogenetic characterization of marine planktonic Archaea in the Santa Barbara Channel. Appllied and Environmental Microbiology 63, 50–56.
Menzel, D., Hopmans, E.C., Schouten, S., Sinninghe Damsté, J.S., 2006. Membrane tetraether lipids of planktonic Crenarchaeota in Pliocene sapropels of the Eastern Mediterranean Sea. Palaeogeography Palaeoclimatology Palaeoecology 239, 1–15.
Mollenhauer, G., McManus, J.F., Benthien, A., Müller, P.J., Eglinton, T.I., 2006. Rapid lateral particle transport in the Argentine Basin: molecular ^{14}C and $^{230}Th_{xs}$ evidence. Deep-Sea Research I 53, 1224–1243.
Mollenhauer, G., Inthorn, M., Vogt, T., Zabel, M., Sinninghe Damsté, J.S., Eglinton, T.I., 2007. Aging of marine organic matter during cross-shelf lateral transport in the Benguela upwelling system revealed by compound-specific radiocarbon dating. Geochemistry Geophysics Geosystems 8, Q09004. http://dx.doi.org/10.1029/2007GC001603.
Mollenhauer, G., Eglinton, T.I., Hopmans, E.C., Sinninghe Damsté, J.S., 2008. A radiocarbon-based assessment of the preservation characteristics of crenarchaeol and alkenones from continental margin sediments. Organic Geochemistry 39, 1039–1045.
Müller, P., Kirst, G., Ruhland, G., von Storch, I., Rosell-Melé, A., 1998. Calibration of the alkenone paleotemperature index $U^{K'}_{37}$ based on core-tops from the eastern South Atlantic and the global ocean (60°°N–60°S). Geochimica et Cosmochimica Acta 62, 1757–1772.
Murray, A.E., Preston, C.M., Massana, R., Taylor, L.T., Blakis, A., Wu, K., DeLong, E.F., 1998. Seasonal and spatial variability of bacterial and archaeal assemblages in the coastal waters near Anvers Island, Antarctica. Applied and Environmental Microbiology 64, 2585–2595.
Murray, A.E., Blankis, A., Massana, R., Strawzewski, S., Passow, U., Alldredge, A., DeLong, E.F., 1999. A time series assessment of planktonic archaeal variability in the Santa Barbara Channel. Aquatic Microbial Ecology 20, 129–145.
Nurnberg, D., Bijma, J., Hemleben, C., 1996. Assessing the reliability of magnesium in foraminiferal calcite as a proxy for water mass temperatures. Geochimica et Cosmochimica Acta 60, 803–814.
Pancost, R.D., Hopmans, E.C., Sinninghe Damsté, J.S., 2001. Archaeal lipids in Mediterranean cold seeps: molecular proxies for anaerobic methane oxidation. Geochimica et Cosmochimica Acta 65, 1611–1627.
Pelejero, C., Grimalt, J.O., 1997. The correlation between the $U^{K'}_{37}$ index and sea surface temperature in the warm boundary: the South China Sea. Geochimica et Cosmochimica Acta 61, 4789–4797.
Pelejero, C., Grimalt, J.O., Heilig, S., Kienast, M., Wang, L., 1999. High-resolution $U^{K'}_{37}$ temperature reconstructions in the South China Sea over the past 220 kyr. Paleoceanography 14, 224–231.
Pitcher, A., Hopmans, E.C., Mosier, A.C., Park, S.J., Rhee, S.K., Francis, C.A., Schouten, S., Sinninghe Damsté, J.S., 2011. Core and intact polar glycerol dibiphytanyl dlycerol tetraether lipids of ammonia-oxidizing archaea enriched from marine and estuarine Sediments. Applied and Environmental Microbiology 77, 3468–3477.
Prahl, F.G., Wakeham, S.G., 1987. Calibration of unsaturation patterns in long-chain ketone compositions for paleotemperature assessment. Nature 330, 367–369.
Qu, T., 2001. Role of ocean dynamics in determining the mean seasonal cycle of the South China Sea surface temperature. Journal of Geophysical Research 106, 6943–6955.
Ravelo, A., Shackleton, N.J., 1995. Evidence for surface-water circulation changes at Site 851 in the eastern tropical Pacific Ocean. Proceedings of the Ocean Drilling Program, Scientific Results 138, 503–514.
Rommerskirchen, F., Condon, T., Mollenhauer, G., Dupont, L., Schefuss, E., 2011. Miocene to Pliocene development of surface and subsurface temperatures in the Benguela Current system. Paleoceanography 26, PA3216. http://dx.doi.org/10.1029/2010PA002074.
Schouten, S., Hopmans, E.C., Pancost, R.D., Sinninghe Damsté, J.S., 2000. Widespread occurrence of structurally diverse tetraether membrane lipids: Evidence for the ubiquitous presence of low-temperature relatives of hyperthermophiles. Proceedings of the National Academy of Sciences of the USA 97, 14421–14426.
Schouten, S., Wakeham, S.G., Sinninghe Damsté, J.S., 2001. Evidence for anaerobic methane oxidation by archaea in euxinic waters of the Black Sea. Organic Geochemistry 32, 1277–1281.
Schouten, S., Hopmans, E.C., Schefuß, E., Sinninghe Damsté, J.S., 2002. Distributional variations in marine crenarchaeotal membrane lipids: a new organic proxy for reconstructing ancient sea water temperatures? Earth and Planetary Science Letters 204, 265–274.
Schouten, S., Forster, A., Panato, E., Sinninghe Damsté, J.S., 2007. Towards the calibration of the TEX_{86} paleothermometer in ancient greenhouse worlds. Organic Geochemistry 38, 1537–1546.
Schouten, S. et al., 2009. An interlaboratory study of TEX_{86} and BIT analysis using high-performance liquid chromatography–mass spectrometry. Geochemistry Geophysics Geosystems 10, Q03012. http://dx.doi.org/10.1029/2008GC002221.
Shah, S.R., Mollenhauer, G., Ohkouchi, N., Eglinton, T.I., Pearson, A., 2008. Origins of archaeal tetraether lipids in sediments: insights from radiocarbon analysis. Geochimica et Cosmochimica Acta 72, 4577–4594.
Shaw, P.-T., Chao, S.-Y., 1994. Surface circulation in the South China Sea. Deep-Sea Research I 41, 1663–1683.
Shevenell, A.E., Ingalls, A.E., Domack, E.W., Kelly, C., 2011. Holocene Southern Ocean surface temperature variability west of the Antarctic Peninsula. Nature 470, 250–254.
Shintani, T., Yamamoto, M., Chen, M.-T., 2011. Paleoenvironmental changes in the northern South China Sea over the past 28,000 years: a study of TEX_{86}-derived sea surface temperatures and terrestrial biomarkers. Journal of Asian Earth Sciences 40, 1221–1229.
Sinninghe Damsté, J.S., Hopmans, E.C., Pancost, R.D., Schouten, S., Geenevasen, J.A.J., 2000. Newly discovered non-isoprenoid glycerol dialkyl glycerol tetraether lipids in sediments. Chemical Communications, 1683–1684.
Sinninghe Damsté, J.S., Hopmans, E.C., Schouten, S., van Duin, A.C.T., Geenevasen, J.A.J., 2002. Crenarchaeol: the characteristic glycerol dibiphytanyl glycerol tetraether membrane lipid of cosmopolitan pelagic crenarchaeota. Journal of Lipid Research 43, 1641–1651.
Sorensen, K.B., Teske, A., 2006. Stratified communities of active archaea in deep marine subsurface sediments. Applied and Environmental Microbiology 72, 4596–4603.
Spang, A., Hatzenpichler, R., Brochier-Armanet, C., Rattei, T., Tischler, P., Spieck, E., Streit, W., Stahl, D.A., Wagner, M., Schleper, C., 2010. Distinct gene set in two different lineages of ammonia-oxidizing archaea supports the phylum Thaumarchaeota. Trends in Microbiology 18, 331–340.
Trommer, G., Siccha, M., van der Meer, M.T.J., Schouten, S., Sinninghe Damsté, J.S., Schulz, H., Hemleben, C., Kucera, M., 2009. Distribution of Crenarchaeota tetraether membrane lipids in surface sediments from the Red Sea. Organic Geochemistry 40, 724–731.
Villanueva, J., Pelejero, C., Grimalt, J., 1997. Clean-up procedures for the unbiased estimation of C_{37} alkenone sea surface temperatures and terrigenous *n*-alkane inputs in paleoceanography. Journal of Chromatography 757, 145–151.

Volkman, J.K., Eglinton, G., Corner, E.D.S., Forsberg, T.E.V., 1980. Long-chain alkenes and alkenones in the marine coccolithophorid *Emiliania huxleyi*. Phytochemistry 19, 2619–2622.

Wakeham, S.G., Lewis, C.M., Hopmans, E.C., Schouten, S., Sinninghe Damsté, J.S., 2003. Archaea mediate anaerobic oxidation of methane in deep euxinic waters of the Black Sea. Geochimica et Cosmochimica Acta 67, 1359–1374.

Wang, P., Li, Q., 2009. The South China Sea. Developments in Paleoenvironmental Research 13. http://dx.doi.org/10.1007/978-1-4020-9745-42 (Springer Science+ Business Media B.V).

Wei, G.J., Deng, W.F., Liu, Y., Li, X.H., 2007. High-resolution sea surface temperature records derived from foraminiferal Mg/Ca ratios during the last 260 ka in the northern South China Sea. Palaeogeography Palaeoclimatology Palaeoecology 250, 126–138.

Wei, Y.L., Wang, J.X., Liu, J., Dong, L., Li, L., Wang, H., Wang, P., Zhao, M.X., Zhang, C.L., 2011. Spatial variations in archaeal lipids of surface water and core-top sediments in the South China Sea and their implications for paleoclimate studies. Applied and Environmental Microbiology 77, 7479–7489.

Weijers, J.W.H., Schouten, S., Hopmans, E.C., Geenevasen, J.A.J., David, O.R.P., Coleman, J.M., Pancost, R.D., Sinninghe Damsté, J.S., 2006a. Membrane lipids of mesophilic anaerobic bacteria thriving in peats have typical archaeal traits. Environmental Microbiology 8, 648–657.

Weijers, J.W.H., Schouten, S., Spaargaren, O.C., Sinninghe Damsté, J.S., 2006b. Occurrence and distribution of tetraether membrane lipids in soils: implications for the use of the TEX_{86} proxy and the BIT index. Organic Geochemistry 37, 1680–1693.

Wong, G.T.F., Ku, T.-L., Mulholland, M., Tseng, C.-M., Wang, D.-P., 2007. The Southeast Asian time-series study (SEATS) and the biogeochemistry of the South China Sea—an overview. Deep-Sea Research II 54, 1434–1447.

Wuchter, C., Schouten, S., Coolen, M.J.L., Sinninghe Damsté, J.S., 2004. Temperature-dependent variation in the distribution of tetraether membrane lipids of marine Crenarchaeota: implications for TEX_{86} paleothermometry. Paleoceanography 19, PA4028. http://dx.doi.org/10.1029/2004PA001041.

Wuchter, C., Schouten, S., Wakeham, S.G., Sinninghe Damsté, J.S., 2005. Temporal and spatial variation in tetraether membrane lipids of marine Crenarchaeota in particulate organic matter: implication for TEX_{86} paleothermometry. Paleoceanography 20, PA3013. http://dx.doi.org/10.1029/2004PA001110.

Wuchter, C., Schouten, S., Wakeham, S.G., Sinninghe Damsté, J.S., 2006. Archaeal tetraether membrane lipid fluxes in the northeastern Pacific and the Arabian Sea: implications for TEX_{86} paleothermometry. Paleoceanography 21, PA4208. http://dx.doi.org/10.1029/2006PA001279.

Zhang, Y.G., Zhang, C.L., Liu, X.L., Li, L., Hinrichs, K.-U., Noakes, J.E., 2011. Methane Index: a tetraether archaeal lipid biomarker indicator for detecting the instability of marine gas hydrates. Earth and Planetary Science Letters 307, 525–534.

Zhao, M.X., Huang, C.-Y., Wang, C.-C., Wei, G.J., 2006. A millennial-scale $U^{K'}_{37}$ sea-surface temperature record from the South China Sea (8°N) over the last 150 kyr: monsoon and sea-level influence. Palaeogeography Palaeoclimatology Palaeoecology 236, 39–55.